Desalination and Water Treatment
www.deswater.com
1944-3994/1944-3986 © 2013 Desalination Publications. All rights reserved
doi: 10.1080/19443994.2012.714856

51 (2013) 1385–1404
February

Taylor & Francis
Taylor & Francis Group

Flow transport modelling of feed species (water and salt) through a seawater RO membrane

Ahmed H. Hashim

Addur SWRO and Ras Abu Jarjur BWRO Desalination Plants, Electricity and Water Authority, Water Production Directorate, Manama, Kingdom of Bahrain
Email: ahhashim@batelco.com.bh

Received 2 March 2012; Accepted 18 July 2012

ABSTRACT

Throughout recent years, there has been various research studies on seawater RO membrane modelling concerned with analysing RO membrane transport theories and touching on significant issues of the unique molecular separation mechanism of reverse osmosis that affect areas of our everyday life. However, much of this research could be largely characterised as being empirical in nature. The scope of this flow transport modelling analysis was to develop a mathematical model that would determine variations in the transport of water (solvent) and salt (solute) species within a seawater RO membrane module during reverse osmosis. Hence, the modelling analysis was performed in terms of flow, pressure and concentration of the seawater feed, whilst traversing through the module from point of entry at the axial–centre along the length of module (travelling as feed) to the point of exit at outer periphery (exiting as retentate). The modelling analysis in this paper has been devised based on a generalised capillary diffusion model for the transport of "water" and "salt" through a seawater RO membrane combined with relevant performance evaluation expressions for a SWRO membrane using actual operating data of a SWRO membrane module. For this purpose, the essential first year operating data for a new seawater RO membrane module (DuPont HFF membrane B-10 6835TR, operated at the Addur SWRO Desalination Plant) were compiled; (Note: the essential operating data for one seasonal year from this new SWRO membrane module were used so as to obtain more accurate results). This modelling analysis work was performed by the Author of this technical paper at the University of Newcastle Upon Tyne in the UK as part of the Author's PhD research work during 2000 (modified in 2007). It is undeniable that concentration polarisation has detrimental effects on the performance of any RO membrane process, with its magnitude being of a vital importance (though not been determined before as no literature cited). Likewise, the resulting concentrated boundary film thickness and salt concentration of boundary solution on the high pressure side of the membrane were also determined in the overall application of this modelling analysis. Thus, the correlations developed for this model, the concept of the generated model and the entirety of merging the expressions (as well as the results achieved) are to provide significance in determining the performance of a seawater RO membrane and to add novelty with a sense of innovation to this modelling work.

Keywords: Water and salt transport through a SWRO membrane; Mathematical model; Transport of water and salt species; SWRO membrane module; RO; Modelling analysis; Concentration polarisation; Concentrated boundary film thickness

Presented at the International Conference on Desalination for the Environment, Clean Water and Energy, European Desalination Society, 23–26 April 2012, Barcelona, Spain

1. Developing the model expressions

The flow transport model expressions developed for this model analysis arise from substantiated RO data analysis involving single solute–aqueous solution systems for all levels of solute separations and isothermal operating conditions [1–3].

Underlying this analysis is the preferential sorption–capillary flow mechanism for reverse osmosis (Fig. 1) [4,5], which implies that the existence and continuous withdrawal of the preferentially sorbed interfacial water through the membrane pores gives rise to a permeate solution (less concentrated than the feed solution) and a more concentrated boundary solution formed between the interfacial region and bulk solution.

In 1956, Sourirajan [6] investigated the possibility of developing a desalination process based on the concept of skimming this monomolecular surface layer of pure water, (whilst further investigation led Sourirajan to determine the existence of a multimolecular layer of pure water at the interface, leading to the conceptual model shown in Fig. 1).

Fig. 1 also represents the recovery of fresh water from saline solution, where saline solution is in contact with a porous membrane (while fresh water is preferen-

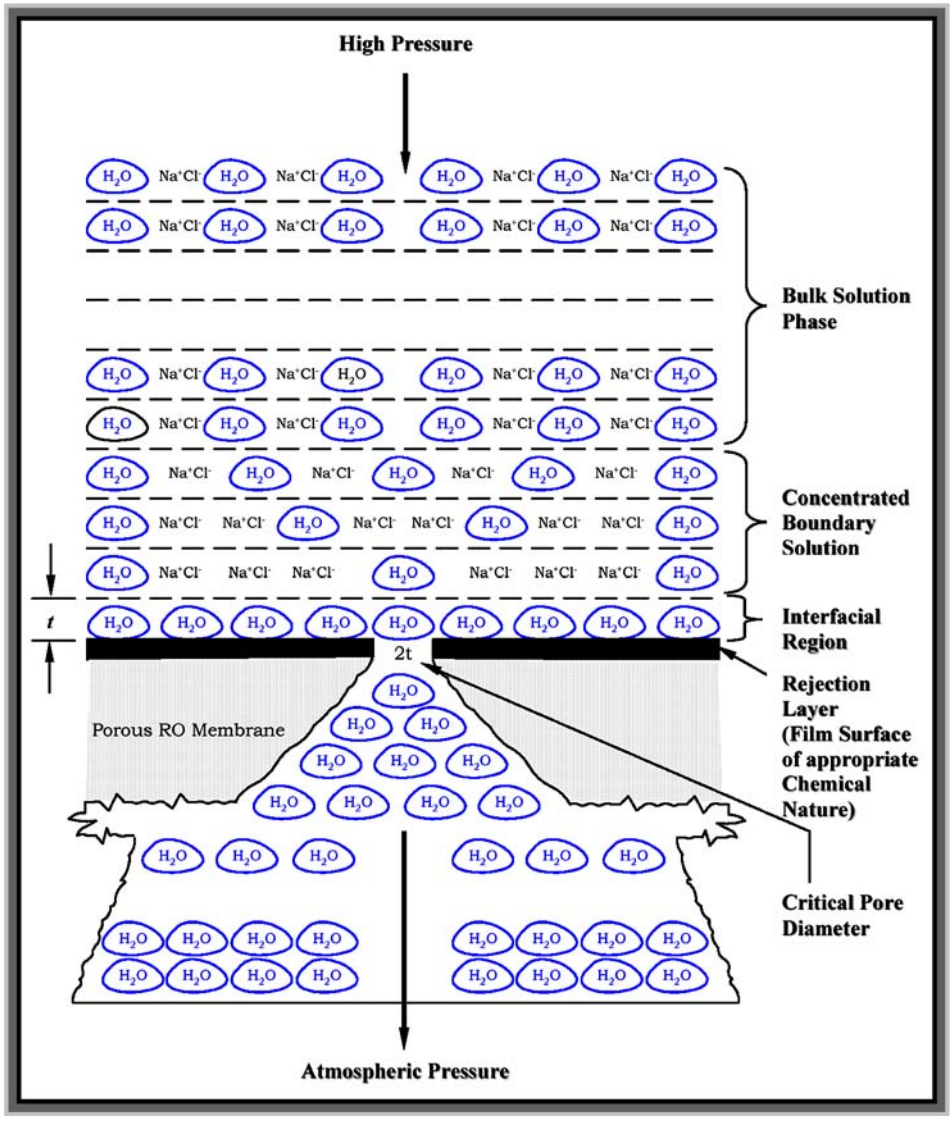

Fig. 1. Schematic representation of preferential sorption–capillary flow mechanism model for RO separations in seawater RO desalination applications.
Source: Adapted from Sourirajan [4,5].

tially sorbed, salt is repelled at the membrane–solution interface by virtue of the chemical nature of the membrane material). This concept eventually led to the practical development of the porous CA and CTA RO membrane intended for seawater desalination.

Fig. 2 [5] is a schematic diagram of a conceptual representation for the transport of feed species during RO under continuous steady state operating conditions.

Under steady state RO operating conditions, three circumstances take place simultaneously: (1) water transport through the membrane pores; (2) salt transport through the membrane pores and (3) mass transfer arising from a concentration gradient between the more concentrated boundary solution and the lesser concentrated bulk solution on the high pressure side of the membrane known as concentration polarisation (which has significant effects on RO membrane performance). Consequently, the modelling analysis of this flow transport model has been developed, whereby each one of these three events is represented with an appropriate transport correlation. By employing the actual process operating data available for the SWRO module under examination, the model analysis shall proceed in the following manner:

- Subscripts "A", "B" and "M" were used in the model to represent "salt", "water" and "membrane phase", respectively.
- Subscripts "1", "2" and "3" were used to represent "bulk (or feed) solution", "concentrated boundary solution" and "membrane permeated solution", respectively.

1.1. Pure water permeability constant, A

Since the pure water permeability rate (or permeation rate) through the effective area of membrane surface ([PWP]) is proportional to the operating gauge pressure (or feed pressure) on the high pressure side of the membrane (P); thus:

$$[\mathrm{PWP}] \propto P \tag{1}$$

An appropriate proportionality constant (represented by the symbol A) can be introduced into Eq. (1) to obtain the following correlation:

$$[\mathrm{PWP}] = AP \tag{2}$$

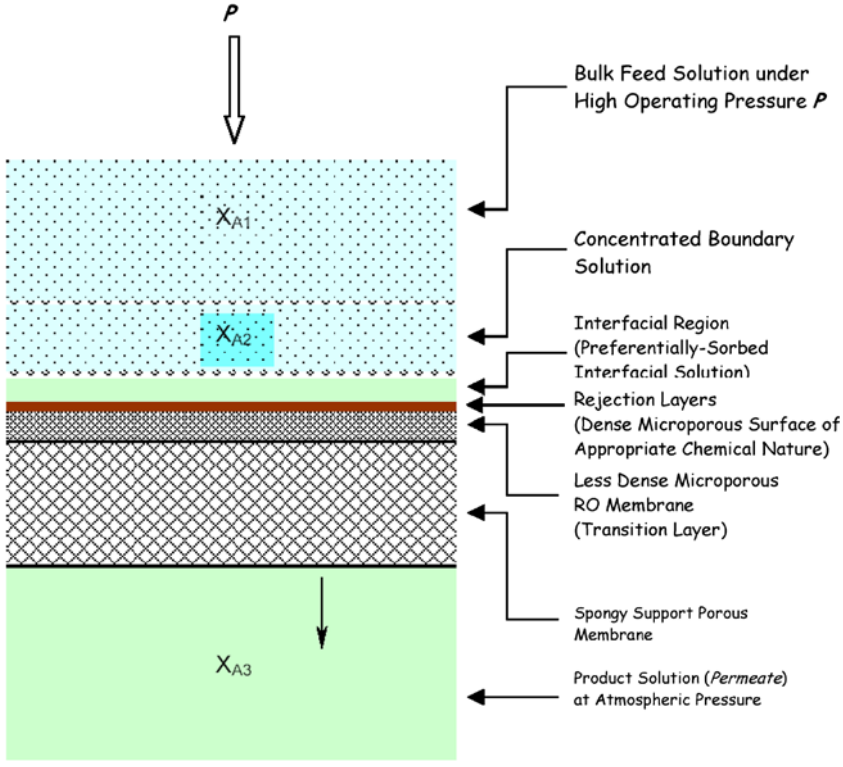

Fig. 2. Schematic of a conceptual representation for the transport of feed species during RO under continuous steady state operating conditions.
Source: Adapted from Sourirajan [5] and modified by the Author of this technical paper.

Thus, the proportionality constant A in Eq. (2) can be defined as [7]:

$$A = \left(\frac{[\mathrm{PWP}]}{M_B \times S \times 3,600 \times P}\right) \quad (3)$$

Note: Eq. (3) defines the pure water permeability constant (A, a fundamental quantity with respect to the RO membrane) with a magnitude independent of any salt under consideration.

1.2. Water flux through the membrane pores, N_B

Water transport through a SWRO membrane is the total water content in the permeated solution, which includes the preferentially sorbed water; hence, water flux through the membrane pores (N_B) is proportional to the effective pressure (ΔP, the driving pressure for water flow through the membrane pores during RO) and the following proportional relationship is applicable:

$$N_B \propto \Delta P \quad (4)$$

The same proportionality constant A is also introduced into Eq. (4) to obtain the following correlation [7]:

$$N_B = A\,\Delta P \quad (5)$$

It is known that with respect to a given membrane–solution system, the magnitude of the interfacial region is a function of the boundary solution concentration [8]; hence, the effective pressure (driving force) for water flow through the membrane surface during RO can be expressed by the following relationship [1,7,9]:

$$\Delta P = P - \Delta\pi \quad (6)$$

$\Delta\pi$ is also defined as:

$$\Delta\pi = \pi_b - \pi_p \quad (7)$$

Note: $\Delta\pi$ (in Eq. (7)) also represents the chemical potential barrier for water transport during RO (which is strictly true only when there is no solute accumulation inside the membrane and solute separation is 100% (i.e. "always positive" and solute is repelled in the vicinity of the membrane surface); hence, Eq. (6) can be rewritten as:

$$\Delta P = P - (\pi_b - \pi_p) \quad (8)$$

Considering this SWRO membrane module case study (while introducing the mole fraction of salt (X_A)), hence, Eq. (8) is re-expressed as in the following correlation:

$$\Delta P = [P - \{\pi(X_{A2}) - \pi(X_{A3})\}] \quad (9)$$

Substituting the expression for ΔP from Eq. (9) into Eq. (5) and simplifying, hence the resulting expression is obtained [7]:

$$N_B = A[P - \pi(X_{A2}) + \pi(X_{A3})] \quad (10)$$

1.3. Salt flux through the membrane pores, N_A

During the seawater RO process, and under steady state operation, there exists a concentration difference on either side of the membrane phase wherein the transport of salt through the membrane phase is treated as owing to pore diffusion [5,7]. In such case, the salt flux through the membrane pores (N_A) is proportional to the difference in salt concentration on either side of the membrane phase; thus, the following proportional relationship applies:

$$N_A \propto (C_{M2}X_{AM2} - C_{M3}X_{AM3}) \quad (11)$$

Note: X_{AM2} and X_{AM3} respectively represent the mole fraction of salt within the membrane phase on both sides of the membrane in equilibrium with X_{A2} and X_{A3} in the solutions phases on either side of membrane (Fig. 3 {analysis by the Author of this technical paper} shows c_{M2} and c_{M3} to represent the molar densities correspond to X_{AM2} and X_{AM3} within the membrane phase, respectively).

An appropriate proportionality constant (represented by the symbol (D_{AM}/δ)) can be introduced into Eq. (11), resulting in the following expression [7]:

$$N_A = \left(\frac{D_{AM}}{\delta}\right)(C_{M2}X_{AM2} - C_{M3}X_{AM3}) \quad (12)$$

Note: Although N_A (solute flux through the membrane pores) can be determined from actual SWRO operating data, in contrast none of the quantities on the right hand side of Eq. (12) is known or could be even precisely measurable (thus, the dividing line between the regions corresponding to X_{AM2} and X_{AM3} within the membrane phase (Fig. 3), if there be any, is also not known and would be only conceptual).

For the benefit of the present modelling analysis, Eq. (12) can be transformed into one containing

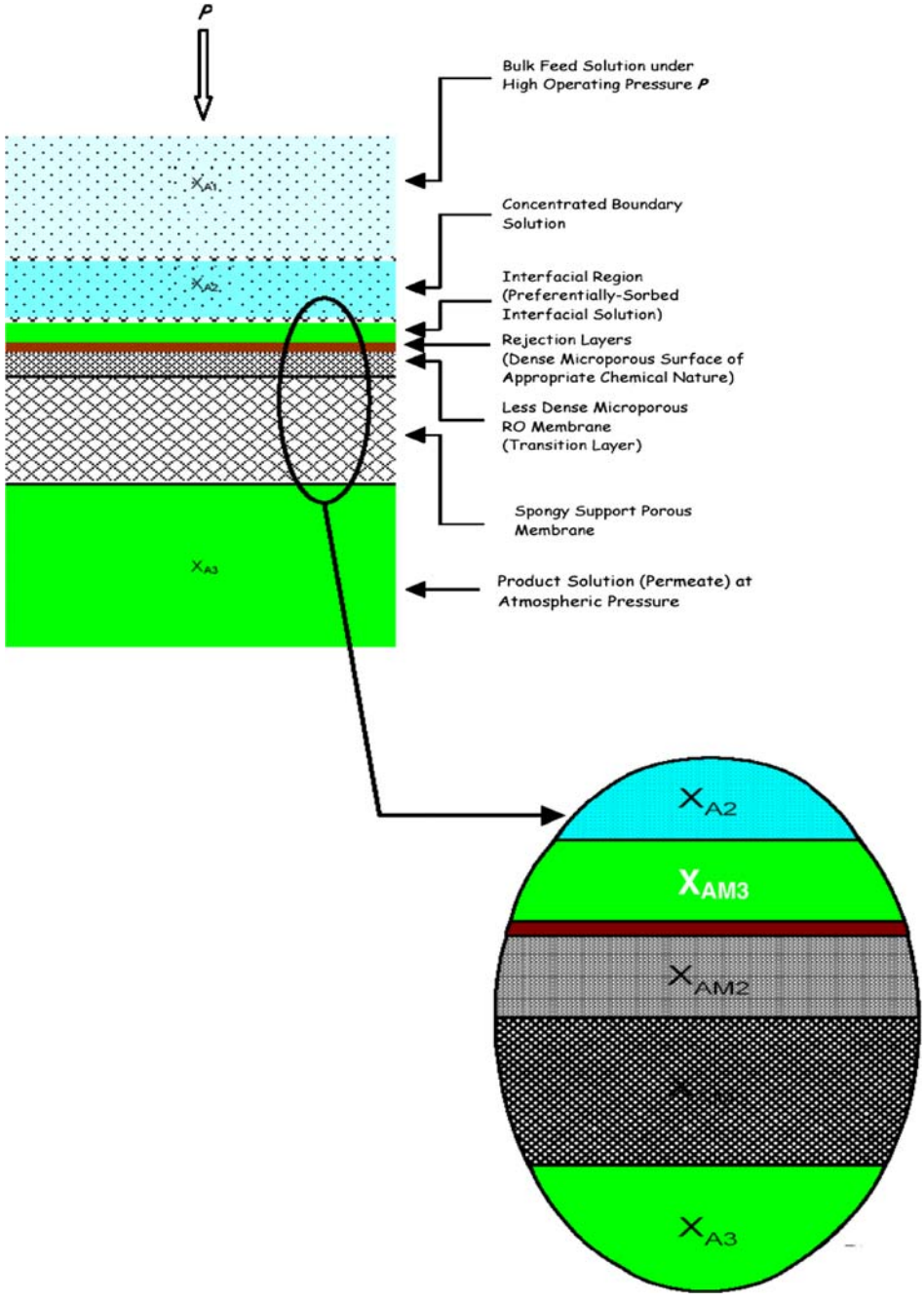

Fig. 3. A schematic to represent the transport of feed species within the membrane phase during the SWRO process under continuous steady state operating conditions.
Source: Adapted from Fig. 2 and modified by the Author of this technical paper (i.e. Author's analyses).

measurable quantities and a group of unknown quantities, which is achieved by assuming a simple linear equilibrium relationship between X_A (concentration of salt in solution phase) and X_{AM} (concentration of salt within membrane phase) [7]:

$$cX_A = K(c_M X_{AM}) \quad (13)$$

Applying Eq. (13) for the equilibrium conditions on each side of the membrane phase, two relations arise:

$$c_2 X_{A2} = K(c_{M2} X_{AM2}) \tag{14}$$

and

$$c_3 X_{A3} = K(c_{M3} X_{AM3}) \tag{15}$$

Blending Eqs. (14) and (15) into Eq. (12), the resulting expression would be:

$$N_A = \left(\frac{D_{AM}}{K\delta}\right)(c_2 X_{A2} - c_3 X_{A3}) \tag{16}$$

Eq. (16) can be also expressed in terms of N_B, since [7]:

$$X_{A3} = \frac{N_A}{(N_A + N_B)} \tag{17}$$

Rearranging Eq. (17) for N_A and N_B; the resulting expressions are as follows:

$$N_A = N_B\left(\frac{X_{A3}}{1 - X_{A3}}\right) \tag{18}$$

and

$$N_B = N_A\left(\frac{1 - X_{A3}}{X_{A3}}\right) \tag{19}$$

By substituting the expression defining N_A from Eq. (16) into Eq. (19), thus, an expression for N_B is obtained:

$$N_B = \left(\frac{D_{AM}}{K\delta}\right)\left(\frac{1 - X_{A3}}{X_{A3}}\right)(c_2 X_{A2} - c_3 X_{A3}) \tag{20}$$

Note: the quantity $(D_{AM}/K\delta)$, the salt transport parameter, is a fundamental quantity for any membrane–solution system; from an RO engineering science standpoint, $(D_{AM}/K\delta)$ is not a mere proportionality constant, it is a combination of several distinct interrelated quantities of important physical significance none of which can be (or need to be) precisely measured for any chemical engineering calculation, and from an RO process design standpoint it is only sufficient to know the overall value of $(D_{AM}/K\delta)$ as it plays the role of mass transfer coefficient with respect to salt transport through the membrane pores [5,7]

1.4. Mass transfer on the high pressure side of the membrane

Since the salt in the concentrated boundary solution also back diffuses into the less concentrated feed solution on the high pressure side of the membrane, a mass transfer coefficient (k, which characterises the RO condition on the high pressure side of the membrane) can be calculated on the basis of the simple film theory. Accordingly, the mass transfer situation on the high pressure side of the membrane can be expressed using the following relation [7,10]:

$$N_A = X_A(N_A + N_B) - D_{AB}\, c_1 \frac{dX_A}{dz} \tag{21}$$

Substituting the expression for N_A from Eq. (17) into the right hand side of Eq. (21) and then by rearranging it the following expression is obtained:

$$\frac{dX_A}{dz} - \frac{(N_A + N_B)}{C_1 D_{AB}} X_A = -\frac{(N_A + N_B)}{C_1 D_{AB}} X_{AB} \tag{22}$$

The boundary conditions characterising Eq. (22) are:

$$\text{when } z = 0: \qquad X_A = X_{A1} \tag{23}$$

and

$$\text{when } z = 1 \qquad X_A = X_{A2} \tag{24}$$

Solving the simple differential relationship expressed in Eq. (22) with respect to the boundary conditions defined by Eqs. (23) and (24) yields the following expression:

$$X_{A2} = X_{A3} + (X_{A1} - X_{A3})\, \exp\left[\frac{(N_A + N_B)}{C_1}\right]\frac{l}{D_{AB}} \tag{25}$$

or

$$\ln\left[\frac{X_{A2} - X_{A3}}{X_{A1} - X_{A3}}\right] = \left[\frac{(N_A + N_B)}{C_1}\right]\frac{l}{D_{AB}} \tag{26}$$

The mass transfer coefficient k on the high pressure side of the membrane is defined in the conventional manner of the film theory [9–11] as:

$$k = \frac{D_{AB}}{l} \quad \text{or} \quad l = \frac{D_{AB}}{k} \tag{27}$$

By substituting the expression for l from Eq (27) into Eq (26), the following correlation is obtained:

$$\ln\left[\frac{X_{A2} - X_{A3}}{X_{A1} - X_{A3}}\right] = \frac{(N_A + N_B)}{c_1 k} \tag{28}$$

Combining Eqs. (17) and (18), the following correlation prevails:

$$(N_A + N_B) = \frac{N_B}{(1 - X_{A3})} \quad (29)$$

Substituting the expression for "$N_A + N_B$" from Eq. (29) into Eq. (28) and rearranging to obtain an expression for N_B:

$$N_B = c_1 k (1 - X_{A3}) \quad \ln\left[\frac{X_{A2} - X_{A3}}{X_{A1} - X_{A3}}\right] \quad (30)$$

1.5. Concentration polarisation modulus on the high pressure side of the membrane, M

The concentration polarisation modulus on the high pressure side of the membrane M is defined as the ratio of the salt concentration in the boundary layer solution (or wall concentration "c_w") to the salt concentration in feed (bulk) solution "c_b". Correspondingly, for the present modelling analysis, M can be represented by the following expression:

$$M = \frac{X_{A2}}{X_{A1}} \quad (31)$$

Note: Evidently, Eq. (31) indicates that as the magnitude of M increases salt flux through the membrane (N_A) increases (since under such condition any solution traversing through the membrane is more concentrated); further, Eq. (31) demonstrates that as X_{A2} can be either be "more than" or "equal to" X_{A1} then M will always be "equal to" 1 or slightly more.

2. Boundary conditions and physicochemical considerations

For this modelling analysis, and in view of the range of solutions concentration involved in the actual SWRO process system of the case under study, it would be appropriate to assume:

2.1. For this model, it is considered that when membrane pore size is only a few times bigger than the size of permeating species (Fig. 1) and the interfacial forces are considerable enough to induce salt separation, water transport through the pores is proportional to the effective driving pressure. Hence, salt transport is owing to pore diffusion and proportional to salt concentration difference across the membrane.

2.2. This model is concerned with "aqueous solution–membrane systems", where water is preferentially sorbed at the membrane–solution interface (where the case under examination represents such system); thus, the transport expressions developed for this model are applicable to systems where the salt is repelled from the membrane surface and there is no salt accumulation inside the membrane pores during RO.

2.3. In this modelling analysis, three assumptions are made: (1) viscous flow for water transport through the membrane; (2) pore diffusion for solute transport through the membrane and (3) film theory for calculating the effective mass transfer coefficient applicable to the concentration polarisation situation on the high pressure side of the membrane.

2.4. The osmotic pressure of any solution ($\pi(X_A)$) under the prevailing operating conditions is, respectively, proportional to the concentration (mole fraction) of the salt in the same solution (X_A, as mg/l); hence, the following proportional relation is proposed:

$$\pi(X_A) \propto X_A \quad (32)$$

Note: Eq. (32) can be developed into a correlation of equivalence involving a factor for converting solution concentration to pressure, which applies for any solution phase within the SWRO membrane system.

Hence, as the "TDS (in mg/l)" can be multiplied by a conversion factor of "6.9×10^{-4}" to obtain the equivalent process pressure in "Bar" (since every "1,000 mg/l" of saline water exerts approximately "0.69 Bar" of osmotic pressure [12]), the following conversion correlation was developed to determine $\pi(X_A)$, in atm, from actual X_A data:

$$\pi(X_A) = X_A \times (6.9 \times 10^{-4}) \times (0.987) \quad (33)$$

2.5. The molar density of a solution (c, in g-mol/cm^3) does not change significantly over a wide range of solute concentration (as this examined case study). For example, the molar density of pure water at 25°C is equal to 5.535×10^{-2} g-mol/cm^3 while that of a 2-molal NaCl–H_2O solution at 25°C is equal to 5.521×10^{-2} g-mol/cm^3.

Hence, for saline solutions within a SWRO system (e.g. seawater feed, bulk or retentate solutions), c is assumed essentially constant within the SWRO membrane module matrix during RO (i.e. $c_1 = c_2 = c_3 = c$, where $c \approx 5.729 \times 10^{-2}$ g-mol/cm^3 (site determined value for seawater at measured seawater density

($\rho = 1.032\,g/cm^3$ at 25°C) for SWRO system at Addur)). Thus, based on this assumption, Eqs. (20) and (30) become:

$$N_B = c\left(\frac{D_{AM}}{k\delta}\right)\left(\frac{1 - X_{AB}}{X_{A3}}\right)(X_{A2} - X_{A3}) \quad (34)$$

and

$$N_B = ck(1 - X_{A3})\ln\left[\frac{X_{A2} - X_{A3}}{X_{A1} - X_{A3}}\right] \quad (35)$$

The mathematical modelling analysis used in this model is general in scope and not limited to any specific feed solution or membrane material.

3. The set of flow transport model equations

From the modelling analysis that preceded and the expressions derived to constitute this flow transport model, eight correlations emerge as the set of equations describing the flow transport of "water" and "salt" species in a seawater RO process that involve binary aqueous solutions and SWRO membranes having preferential sorption for water during the actual seawater RO process. These eight correlations are: Eqs. (3), (9), (10), (18), (27), (31), (34) and (35):

Out of this set of equations, four correlations (i.e. Eqs. (3), (10), (34) and (35)) together considered the principal correlations that simultaneously govern RO transport as the one entire set of equations to constitute the flow transport within an SWRO membrane system, involving preferential sorption for water at the membrane–solution interface.

4. Application of model

The model developed in this technical paper for the flow transport of water and salt species within the seawater feed was applied to the case study in hand, which involves a new SWRO membrane module (DuPont B-10 (PA HFF configuration)) operated in seawater desalination at the Addur Plant with the seawater feed solution being analogous to the system NaCl–H_2O.

4.1. Parameters determined through applying the model equations

The primary operating data available from the SWRO system were used in the flow transport model equations and systematically applied in the following sequence to obtain the appropriate value of the principal parameters and quantities that will follow:

4.1.1. Eq. (3) was applied to yield values for A (pure water permeability constant), where values for [PWP], S and P were calculated from actual operating data (while $M_B = 18.015$, refer to Nomenclature).

4.1.2. Eq. (10) enables to calculate $\pi(X_{A2})$ (osmotic pressure of the concentrated boundary solution on the high pressure side of the membrane; hence, determining X_{A2} (solute concentration (mole fraction) of the boundary solution) for the prevailing operating conditions.

Note: values for N_B (water flux through membrane pores) and $\pi(X_{A3})$ (osmotic pressure of permeate on the low pressure side of the membrane) corresponding to X_{A3} (salt concentration (mole fraction) of permeate for the prevailing operating conditions) are calculated from actual operating data.

4.1.3. Eq. (34) determines the quantity ($D_{AM}/K\delta$) (solute transport parameter); the value for c (molar density of the solution) was identified in Section 2 (2.5).

4.1.4. Eq. (35) yields k (mass transfer coefficient on the high pressure side of the membrane) applicable to the prevailing operating conditions; values for X_{A1} (salt concentration (mole fraction) of the feed (bulk) solution on the high pressure side of the membrane) for the prevailing operating conditions were calculated from actual operating data.

4.1.5. Eq. (18) was applied to determine N_A (salt flux through the membrane).

4.1.6. Eq. (31) was applied to determine M (magnitude of concentration polarisation modulus on the high pressure side of the membrane).

4.1.7. Eq. (27) was applied to determine l (concentrated solution film (or boundary layer) thickness); the value for D_{AB} (diffusivity of salt in water) relevant to the examined SWRO membrane has been defined in Section 4.4.2).

4.1.8. Eq. (9) used to calculate ΔP (effective pressure values applicable to the examined SWRO system).

4.2. Parameters determined through applying actual operating data

There are essential parameters applicable to the examined SWRO system that need to be determined directly from actual operating data (the values of

which were then applied in the flow transport model equations); they were: [PWP], S, N_B and π (X_{A3}).

4.2.1. [PWP] (pure water permeability rate (permeation rate) through the effective area of the RO membrane surface) can be determined using the correlation proposed below:

$$[\text{PWP}] = \left(\frac{Q_1 \times 10^6}{RS_B/100}\right) \tag{36}$$

Notes: (1) Q_1 represents the volumetric feed flow rate for a single SWRO membrane module (in m^3/h); (2) RS_B represents the rate of water separation or conversion (in%); and 3) 10^6 is the unit conversion factor to obtain [PWP] (in g/h).

4.2.2. S represents the effective area of membrane surface (in cm^2), where the membrane fibre bundle design surface area is available for B-10 (6835TR Type) as 424 m^2 (or 4,564 ft^2) [13]. Now, the correlation expressed by Eq. (37) is an expression modified from a derived correlation [14] to a proposed expression with which S can be calculated in cm^2:

$$S = [424 - (0.093 \times day)] \times 10^4 \tag{37}$$

Notes: (1) Eq. (37) was derived in Ref. [14] to define A_t (realistic predicted value for the surface area of membrane fibre bundle at any operating time t) to consider variations in the actual value of membrane surface area; since S and A_t are one and the same, hence the equation was modified to an expression for S; (2) *day* represents the RO membrane operating day; and (3) 10^4 is the unit conversion factor to obtain S in cm^2.

4.2.3. N_B is determined using the correlation proposed below:

$$N_B = \left(\frac{Q_3 \times 10^6}{S \times M_B \times 3,600}\right) \tag{38}$$

Notes: (1) Q_3 represents the volumetric permeate flow rate for one single SWRO membrane module (m^3/h); and 2) 10^6 is a unit conversion factor

4.2.4. $\pi(X_{A3})$ is determined using the "solution concentration to pressure" conversion correlation proposed below:

$$\pi(X_{A3}) = X_{A3} \times (6.9 \times 10^{-4}) \times 0.987 \tag{39}$$

4.3. Available primary SWRO operating data

There are various process operation data available from the actual SWRO system being examined; however, only a selection of fundamental data is considered as primary for this flow transport modelling analysis. The most relevant parameters of concern from the actual process data are: Q_1, RS_B, P, Q_3, X_{A3} and X_{A1}; for convenience of calculations, values of these parameters (i.e. "available" and "calculated from available") were selected when the operation became more stabilised, as illustrated in Table 1.

4.4. Relevant design and feed water parameters

There are also some design and feed water relevant parameters related to the SWRO system being examined essential to the flow transport model calculations: *S-Design*, D_{AB} and m:

4.4.1. *S-Design* is the design surface area of the SWRO membrane bundle (=424 m^2 [15]).

4.4.2. D_{AB} is the diffusivity of salt in the seawater feed solution = 1.475×10^{-5} cm^2/s (calculated from data available in the literature [16] for the System NaCl–H_2O at 25°C, at seawater solute molality (m) of 0.550 [17]).

4.4.3. m is the solute molality in the seawater feed solution (obtained from data available in the literature [17] for properties of seawater at 25°C as 0.550).

5. Analysis of main results

5.1. Primary results achieved (an example of one set of calculation steps)

The flow transport model equations and correlated expressions developed for this model were employed to demonstrate one set of calculation steps (as illustrated for each principal parameters) using the most relevant primary operating data from the SWRO system under study for one day selected at initial operation stage when the system became stabilised. The eight principal parameters analysed were: A, X_{A2}, $(D_{AM}/K\delta)_{SW}$, k_{SW}, N_A, M, l and ΔP.

To determine the full set of values for these eight principle flow transport model parameters, the one day set of calculation steps were repeated for the whole period of the SWRO system operation using

Table 1
The most relevant parameters of concern (i.e. "available" and "calculated from available") from the actual process operating data selected when system operation became stabilised

Q_1	1.953	m^3/h	Calculated
RS_B	34.851	%	Calculated
P	6,331–63.31–62.481	kPa—Bar—atm	Available in kPa
Q_3	0.681	m^3/h	Calculated
X_{A3}	361.4–0.036	As mg/l—as Wt.%	Calculated
X_{A1}	57,677.030–5.768	As mg/l—as Wt.%	Calculated

Note: An example of calculation: Q_1: feed flow rate for single RO module = feed flow rate/number of modules = 703/360 = 1.953 m^3/h. RS_B: rate of separation or conversion rate = (permeate flow rate/feed flow rate) × 100 = (245/703) × 100 = 34.851%. Q_3: permeate flow rate for single RO module = permeate flow rate/number of modules = 245/360 = 0.681 m^3/h. X_{A3}: concentration of permeate = permeate electrical conductivity (in μS/cm) × conversion factor for permeate = 695/0.52 = 361.4 mg/l = 361.4/10,000 = 0.0361 Wt.% X_{A1}: concentration of bulk solution* = ("feed + retentate" TDS (in mg/l))/2 = 57,677.03 mg/l = 5,768 Wt.%. Note: *: X_{A3} = permeate solution salinity (or salt concentration (mole fraction) of permeate) and X_{A1} = feed (bulk■) solution salinity on the high pressure side of the membrane for the prevailing operating conditions; (■: during RO, feed and retentate solutions contained in the module as together constitute the bulk solution; thus, it is appropriate to consider an overall homogeneity of solutions within the module and bulk solution concentration represents the average feed/retentate concentrations).

MS Excel (when needed, appropriate unit conversions were applied). Thus, many of the following charts were generated to illustrate the profile trends of all the eight principal parameters for the whole period during the case study operation.

5.1.1. A (pure water permeability constant)

The pure water permeability constant was calculated in three primary steps:

Step 1: [PWP] calculated using Eq. (36) at $Q_1 = 1.953$ m^3/h (Table 1) and $RS_B = 34.851\%$ to equal $\approx 5.603 \times 10^6$ g/h.
Step 2: S calculated using Eq. (37) to equal 4,233,490 cm^2 and
Step 3: A hence determined by applying model Eq. (3) at $M_B = 18.015$ and $p = 62.481$ atm (Table I) to equal $\approx 3.203 \times 10^{-7}$ g-mol-H_2O/cm^2 s atm.

The above calculation steps were repeated for the whole number of days of the SWRO membrane module system operation, hence Fig. 4 was generated.

The significance of Fig. 4 comes into view when appreciating that the quantity A is a measure of the overall porosity of membrane in terms of permeation rate of pure water for which the membrane material has preferential sorption from bulk solution during RO. The quantity A represents the pure water transport in the absence concentration polarisation and reflects the compaction effects that asymmetric polymeric porous membranes are subjected to at the prevailing operating system pressure.

Fig. 4 shows that A had a generally steady trend except for the sudden increase between 5,200 and 6,200 h that seemed to respond sharply with rise in seawater feed temperature. Thus, variation in A values was analysed against changes in seawater feed temperature (illustrated Fig. 5) and the results are shown in Fig. 14 (Section 6).

5.1.2. X_{A2} (salt concentration (mole fraction) of the boundary solution)

The salt concentration of the boundary solution on the high pressure side of the SWRO membrane was calculated in four primary steps:

Step 1: N_B calculated using Eq. (38) at $Q_3 = 0.681$ m^3/h (Table 1) to equal $\approx 2.479 \times 10^{-6}$ g-mol/cm^2 s;

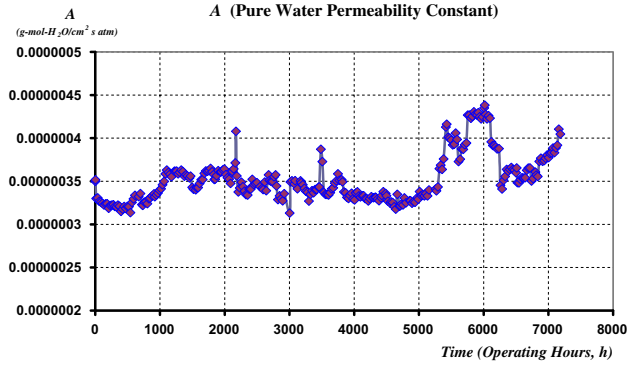

Fig. 4. Pure water permeability constant (A) profile trend.

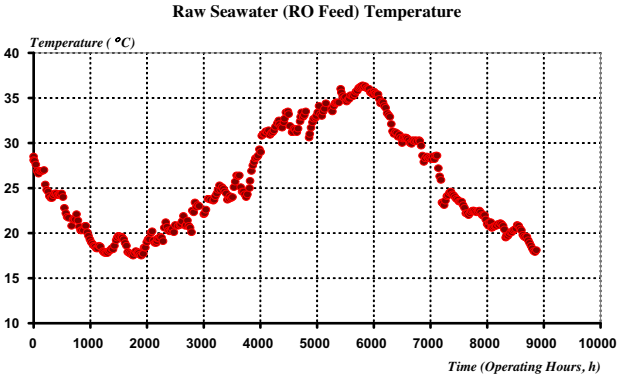

Fig. 5. Chlorinated raw seawater (RO feed) temperature profile trend.
Note: In SWRO desalination, seawater temperature is known to play a vital role in influencing complexity of the constituents in raw seawater and in orchestrating many chemical and process parameters (e.g. activity of organic/inorganic matter, SDI, turbidity, coagulation/flocculation efficiency as well as having an effect on several RO parameters).

Step 2: $\pi(X_{A3})$ calculated using Eq. (39) at $X_{A3} = 361.4$ mg/l (Table 1) to equal ≈ 0.2461 atm;

Step 3: $\pi(X_{A2})$ determined by applying model Eq. (10) at $A \approx 3.203 \times 10^{-7}$ g-mol-H_2O/cm^2 s atm (determined earlier using Eq. (3)) to equal ≈ 55.138 atm and

Step 4: X_{A2} hence determined using the correlation expressed by Eq. (33), modified for X_{A2}, to equal $\approx 80{,}971$ mg/l (or 8.097 Wt.%).

The calculation steps were repeated for the whole number of days of the SWRO membrane module system operation to generate Fig. 6.

Fig. 6 illustrates the profile trend of X_{A2}, which is a significant and unique quantity in RO; it represents the degree of salt concentration within the boundary solution caused by concentration polarisation developing close to the RO membrane surface on the high pressure side of the membrane during RO. The X_{A2} data in Fig. 6 seemed to have a certain response to higher levels seawater feed temperature (from Fig. 5), analysed in Fig. 15 (Section "VI").

5.1.3. $(D_{AM}/K\delta)_{SW}$ (solute (salt) transport parameter for the seawater feed)

This parameter was determined by applying model Eq. (34) at $c = 5.729 \times 10^{-2}$ g-mol/cm^3, $X_{A2} \approx 8.097$ Wt.% (determined earlier using Eq. (33))

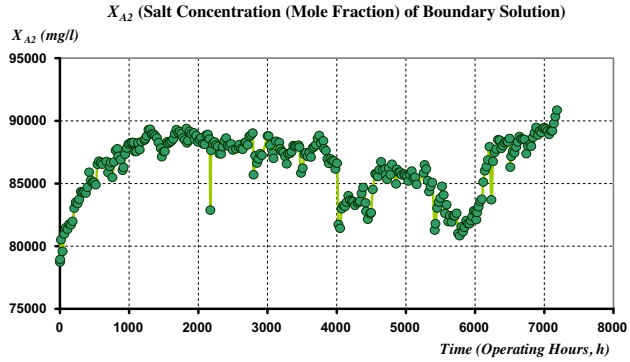

Fig. 6. Salt concentration (mole fraction) of the boundary solution (X_{A2}) profile trend.

and $X_{A3} = 0.036$ Wt.% (Table 1) to equal $\approx 2.013 \times 0^{-7}$ cm/s.

The above calculation was repeated for the whole number of days of the SWRO membrane module system operation to generate Fig. 7.

Fig. 7 illustrates the profile of the unique quantity $(D_{AM}/K\delta)_{SW}$ (salt transport parameter), which has the significance for being a function of chemical nature of salt, membrane material and average pore size on membrane surface, reflecting the equilibrium and kinetic effects governing seawater RO transport. A relatively lower $(D_{AM}/K\delta)_{SW}$ indicates a relatively smaller average pore size (this is to say a membrane with relatively lower $(D_{AM}/K\delta)_{SW}$ for a salt indicates a less salt transport through the membrane, thus results in a higher salt separation in RO).

A closer comparison of the results obtained for the quantity $(D_{AM}/K\delta)_{SW}$ in Fig. 7 against other parameters from actual operating data (e.g. N_A (salt flux through the SWRO membrane), Fig. 9) indicates that there exist unique relationships of an exact trend while there exists an inverse relationship with salt rejection (some relationships were graphically analysed in Section 6).

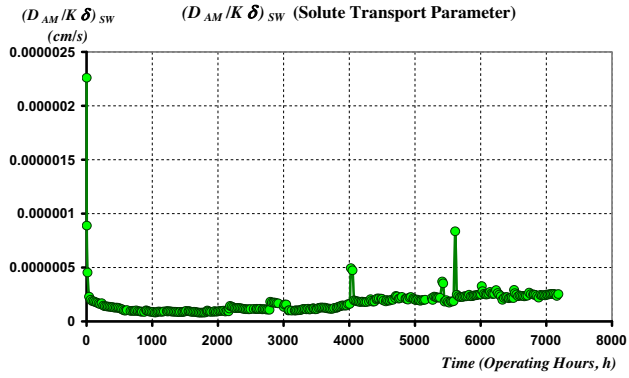

Fig. 7. Solute (salt) transport parameter for the seawater feed solution ($(D_{AM}/K\delta)_{SW}$) profile trend.

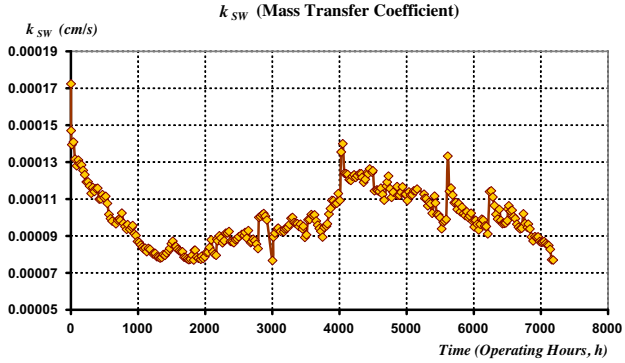

Fig. 8. Mass transfer coefficient for the seawater feed solution (k_{SW}) profile trend.

5.1.4. k_{SW} (mass transfer coefficient for the seawater feed)

This parameter was determined by applying model Eq. (35) at $X_{A1} \approx 5.768$ Wt.% (Table 1) to equal $\approx 1.316 \times 10^{-4}$ cm/s.

The above calculation was repeated for the whole number of days of the SWRO membrane module system operation to generate Fig. 8.

The quantity k_{SW} represents the mass transfer coefficient for seawater feed solution, which has a fundamental significance for being concerned with the salt within the concentrated boundary solution as it back diffuses into the less concentrated feed solution thereby establishing the concentration polarisation situation (represented by the ratio "X_{A2}/X_{A1}"). The magnitude of k_{SW} is a function of nature of salt, salt concentration in feed solution (X_{A1}) and feed flow rate (or degree of turbulence) on the high pressure side of the membrane.

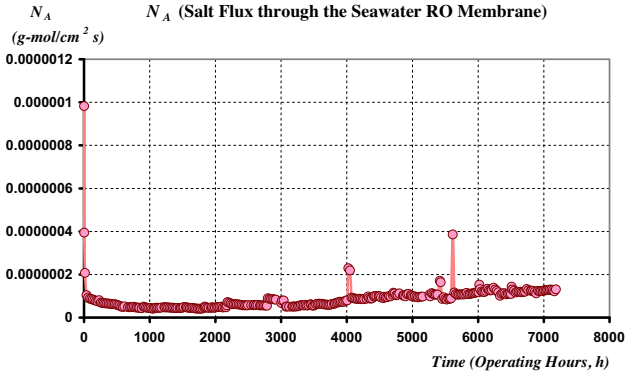

Fig. 9. Salt flux through the SWRO membrane (N_A) profile trend.

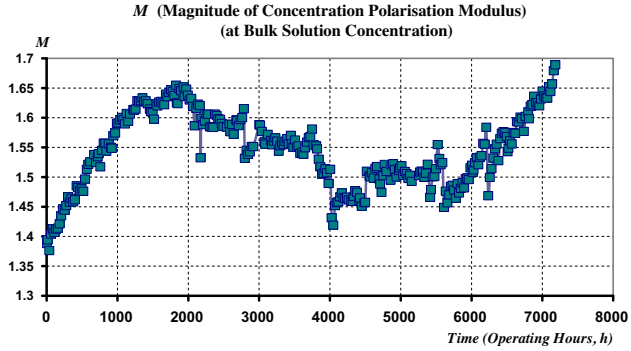

Fig. 10. Magnitude of the concentration polarisation modulus (M, at bulk solution concentration) profile trend.

5.1.5. N_A (salt flux through the SWRO membrane)

The N_A parameter was determined by applying model Eq. (18) to equal $\approx 9.294 \times 10^{-8}$ g-mol/cm^2 s. The above calculation was repeated for the whole number of days of the SWRO membrane module operation to generate Fig. 9.

A closer comparison of the results obtained for the quantity N_A profile shown in Fig. 9 against that of the quantity $(D_{AM}/K\delta)_{SW}$ (salt transport parameter) illustrated in Fig. 7 indicates a unique relationship between the two parameters (both results were graphically analysed against each other in Section 6).

5.1.6. M (magnitude of concentration polarisation modulus)

M was determined by applying model Eq. (31) to equal ≈ 1.404. The calculation was repeated for the whole number of days for the SWRO membrane module system operation to generate Fig. 10.

Fig. 10 illustrates the magnitude of the quantity M determined through the developed modelling

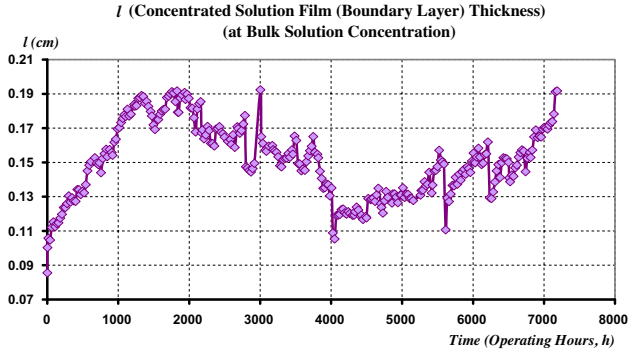

Fig. 11. Concentrated solution film (boundary layer) thickness (l, at bulk solution concentration) profile trend.

analysis, which has significant implications in RO and considerable consequences on RO membrane performance.

The varying magnitude of M was analysed against the results obtained for X_{A2} (salt concentration of boundary solution at the high pressure side of the membrane surface), k_{SW} (mass transfer coefficient for the seawater feed) and l (concentrated solution film thickness on the high pressure side of the membrane), as illustrated in Section 6.

5.1.7. l (concentrated solution film (boundary layer) thickness on the high pressure side of the membrane)

l was determined by applying model Eq. (27) at $D_{AB} = 1.475 \times 10^{-5}$ cm^2/s (determined in Section 4.4.2) and $k_{SW} \approx 1.316 \times 10^{-4}$ cm/s (determined using Eq. (35)) to equal 0.112 cm. The calculation was repeated for the whole number of days for the SWRO membrane module system operation to generate Fig. 11.

Fig. 11 shows the measure of the quantity l calculated through the developed modelling analysis, which is a significant parameter of considerable influence on the RO membrane performance during reverse osmosis.

The varying magnitude of l was analysed against the results obtained for X_{A2} (salt concentration of boundary solution at the high pressure side of the membrane surface), k_{SW} (mass transfer coefficient for the seawater feed) and M (the concentration polarisation modulus), as illustrated in Section 6.

5.1.8. ΔP (effective pressure)

This parameter was determined by applying model Eq. (9) at $\pi(X_{A2}) \approx 55.138$ atm (determined using Eq. (10)) and $\pi(X_{A3}) \approx 0.2461$ atm (determined using Eq. (39)) to equal 7.589 atm.

This calculation was repeated for the whole number of days of the SWRO membrane module system operation to generate Fig. 12.

Fig. 12 displays the values of ΔP (effective pressure during RO under the prevailing operating conditions) calculated through the developed modelling analysis, which is a significant parameter of considerable effect on the RO membrane separation process.

The fluctuating values of ΔP was analysed against changes in seawater feed temperature from Fig. 5, as illustrated in Fig. 28 in Section 6.

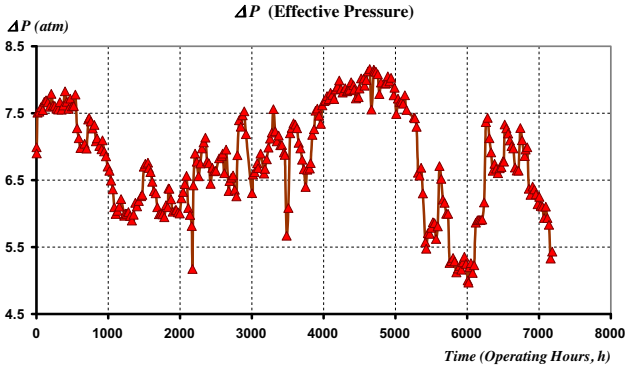

Fig. 12. Effective pressure (ΔP) profile trend.

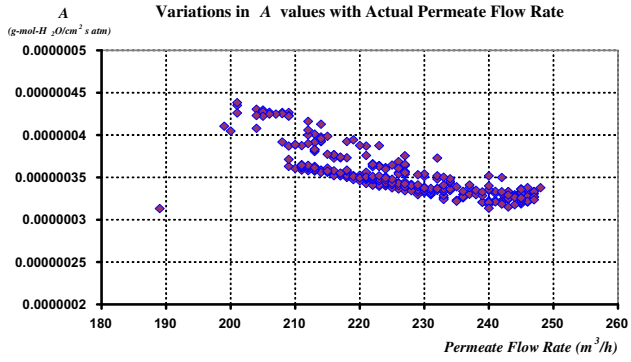

Fig. 13. Variations in pure water permeability constant (A) with changes in actual permeate flow rate.

6. Investigative analysis of model results

The principal parameters derived and calculated through this model (i.e. A, X_{A2}, $(D_{AM}/K\delta)_{SW}$, k_{SW}, M and l) are fundamental quantities with respect to the SWRO process and valid for the examined SWRO membrane module and prevailing operating conditions.

All these quantities are unique, especially those relevant to the concentrated boundary solution on the

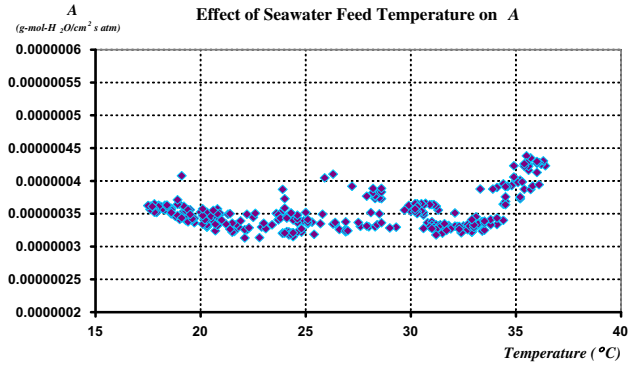

Fig. 14. Effect of seawater feed temperature on the pure water permeability constant (A).

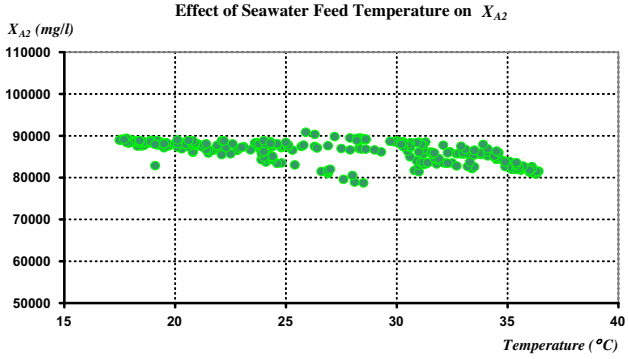

Fig. 15. Effect of seawater feed temperature on the salt concentration of the boundary solution at the high pressure side of the membrane surface (X_{A2}).

high pressure side of the RO membrane (i.e. X_{A2}, M and l), and have not been determined for a SWRO system (no literature cited).

6.1. A

Because of its relevance to permeate flow rate, variations in A values (from Fig. 4) were examined against those of actual permeate flow rate for the SWRO membrane system under study and the results are illustrated in Fig. 13.

The results in Fig. 13 show that pure water permeability constant had an overall decreasing trend relationship with that of actual permeate flow rate, which would most probably attributed to raw seawater seasonal and temperature changes throughout the operation of the SWRO membrane module being examined.

Fig. 14 shows the variation in the values of A analysed against changes in seawater feed temperature (from Fig. 5).

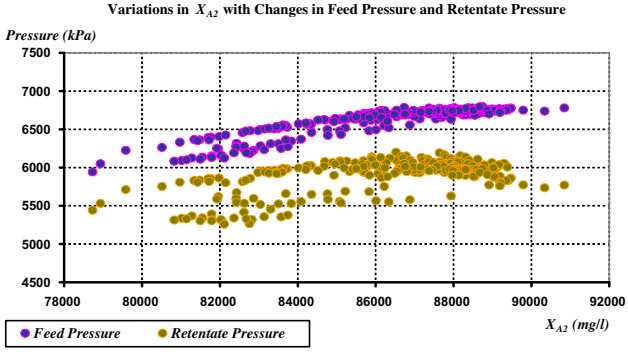

Fig. 16. Variations in salt concentration of the boundary solution at the high pressure side of the membrane surface (X_{A2}) with changes in feed pressure and retentate pressure.

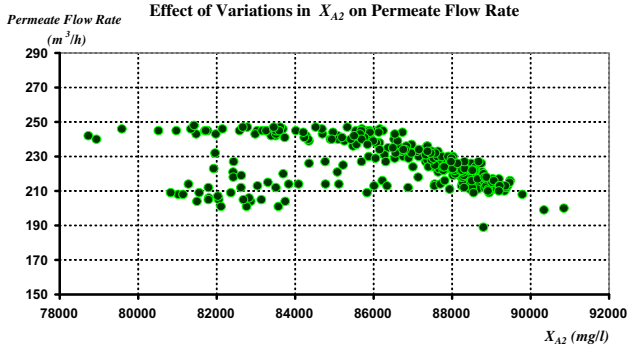

Fig. 17. Effect of the variations in X_{A2} values on the permeate flow rate.

As mentioned in Section 5.1.1, Fig. 14 showed sudden increase in the pure water permeability constant "A" values between 5,200 and 6,200 h of operation. Now, Fig. 14 reveals that the sharp increase in A values transpired when seawater feed temperature increased above 34°C, which indicate that the overall porosity of the SWRO membrane under study significantly increased at this higher seawater feed temperature.

6.2. X_{A2}

Values of the quantity X_{A2} (salt concentration of the boundary solution at the high pressure side of the membrane surface), from Fig. 6, were analysed against seawater feed temperature (from Fig. 5); the results are illustrated in Fig. 15.

Fig. 15 shows a reasonably steady profile trend of the salt concentration of the boundary layer (X_{A2}) that encountered a meek declined in value when the seawater feed temperature climbed to above 34°C. This indicates that the magnitude of the salt concentration of the boundary solution at the high pressure side of the membrane (represented by X_{A2}) at the prevailing operating conditions of the SWRO system under study moderately lowered at a higher seawater feed temperature (a lower X_{A2} also indicates a lower M, because X_{A2} is a consequence of M).

Since the quantity X_{A2} has considerable relevance to the feed pressure and retentate pressure of the SWRO system, the effect of these two pressure parameters (from actual data of the SWRO system under study) was analysed against the values of the quantity X_{A2} from Fig. 6 (as illustrated in Fig. 16).

Fig. 16 indicated that X_{A2} had a clear linear relationship with changes in feed pressure and retentate pressure. This affirms that any rise in pressure on the high pressure side of the membrane causes a drastic build-up of salt concentration at the membrane

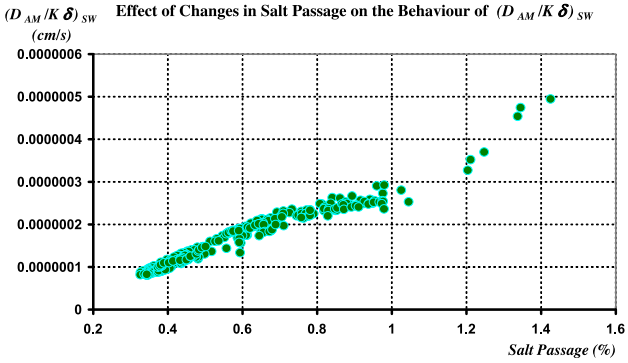

Fig. 18. Effect of the changes in salt passage on the behaviour of $(D_{AM}/K\delta)_{SW}$.

surface, which affects the concentration polarisation modulus (M) magnitude and thickness of the boundary concentration film on the high pressure side of the membrane (l).

In addition, the effect of variations in X_{A2} on permeate flow rate of the SWRO system (from actual data of SWRO system under study) was also examined in Fig. 17, which showed a very distinctive finding. The results indicated that during the SWRO process, the X_{A2} values kept on continuously increasing while the permeate flow rate remained essentially constant; however, when X_{A2} reached a value of around 86,000 mg/l the permeate flow rate began persistently dropping up to the end of the study period.

This phenomenon can be explained by the fact that when X_{A2} attained a value of about 86,000 mg/l (and beyond) it began affecting (or retarding) the permeate flow rate acting as a barrier hindering the flow of pure water through the RO membrane.

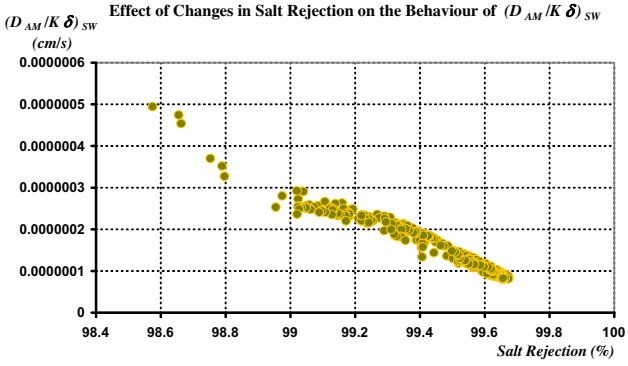

Fig. 19. Effect of the changes in salt rejection on the behaviour of $(D_{AM}/K\delta)_{SW}$.

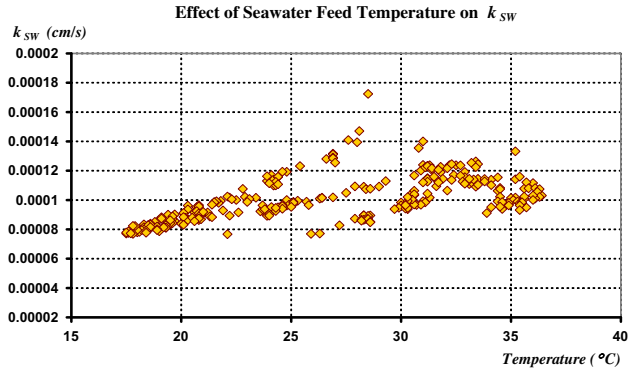

Fig. 20. Effect of seawater feed temperature on the mass transfer coefficient for the seawater feed (k_{SW}).

6.3. $(D_{AM}/K\delta)_{SW}$

In reference to Section 5.1.3, the results obtained for the quantity $(D_{AM}/K\delta)_{SW}$ (salt transport parameter) from Fig. 7 were analysed against the profile data of salt passage (owing to their unique resemblance in trends) and the profile data of salt rejection (owing to their unique reverse resemblance in trends), both from actual data of SWRO system under study.

These two relationships are graphically presented in Figs. 18 and 19, respectively, where they indicate that there exist unique linear relationships of an exact opposite to each other. This is most comprehensible since these three parameters are directly concerned with the salt content within the solution matrix contained in the RO module.

Analysing these findings, it becomes apparent that the salt transport intensity through the SWRO membrane (represented by $(D_{AM}/K\delta)_{SW}$) increases with the

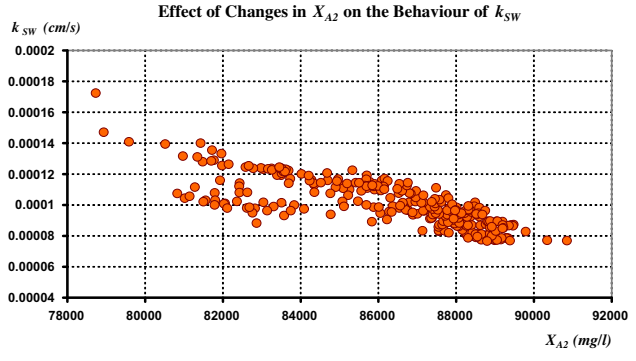

Fig. 21. Effect of changes in salt concentration of the boundary solution at the high pressure side of the membrane surface (X_{A2}) on the behaviour of mass transfer coefficient for the seawater feed (k_{SW}).
Note: When $k = \infty$, $X_{A2} = X_{A1}$, and for all finite values of k, X_{A2} is > X_{A1} and concentration polarisation situation is best expressed by a numerical value for k, which is correlated to actual feed flow (or turbulence conditions) on the high pressure side of the membrane.

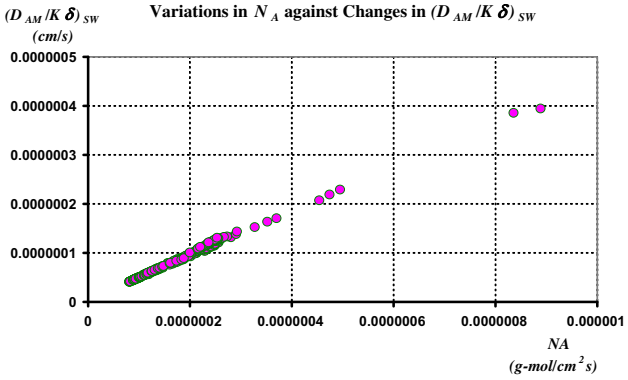

Fig. 22. Variations in N_A (salt flux through the SWRO membrane) against $(D_{AM}/K\delta)_{SW}$ (salt transport parameter).

increase in salt passage (as indicated by Fig. 18) and reduces with the increase in salt rejection (as indicated by Fig. 19). This is an expected tendency during a typical RO process, authenticating further the validity of the flow transport model developed in this chapter.

6.4. k_{SW}

Variations in the quantity k_{SW} values from Fig. 8 were analysed against changes in seawater feed temperature from Fig. 5; the results are illustrated in Fig. 20.

The linear relationship that exists between mass transfer coefficient for seawater feed (k_{SW}) and seawater feed temperature (as indicated by Fig. 20) underlines the mass transfer coefficient tendency to increase with increase in seawater feed temperature, because the water flux through the membrane pores (N_B, an essential parameter (Eqs. (34) and (35)) increases with the increase in seawater feed temperature.

This asserts more the linear effect of seawater feed temperature on relative pore size of the RO membrane.

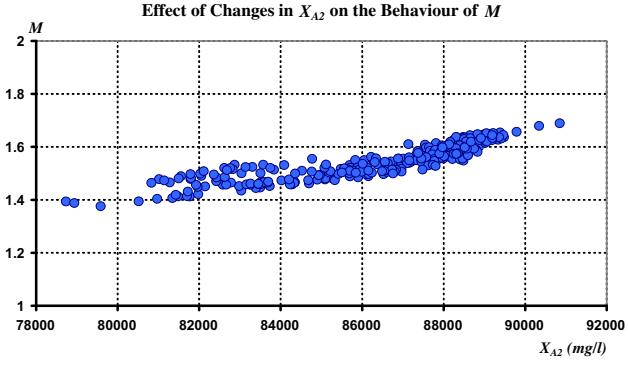

Fig. 23. Effect of changes in salt concentration of boundary solution at the high pressure side of the membrane surface (X_{A2}) on the behaviour of the concentration polarisation modulus (M).

The profile trend in Fig. 20 also illustrates a distinct behaviour of the quantity k_{SW} occurring between the seawater feed temperature range 25–30˚C that suggests three independent linear relationships. This is attributed to the rhythmic (cyclic) seasonal rise and fall in seawater feed temperature during the study period. Looking at the profile trend in Fig. 5, it shows that there were "two falls" and "one rise" in seawater feed temperature that explains this curious behaviour for k_{SW} magnitude, which again relates to the resulting water flux through the membrane pores (N_B) during this period.

The effect of changes in the X_{A2} values was studied against the behaviour of k_{SW} where it appeared to have an inversely proportional relationship, as illustrated in Fig. 21.

Fig. 21 indicates that (also in reference to Fig. 17) as the salts within the boundary solution at the high pressure side of the membrane grew in concentration (i.e. higher X_{A2}). the mass transfer coefficient (which impeded the pure water flow through the membrane surface) became affected.

6.5. N_A

As discussed in Section 5.1.5, the results obtained for the quantity N_A (salt flux through the SWRO membrane, Fig. 9) were analysed against that of the quantity $(D_{AM}/K\delta)_{SW}$ (salt transport parameter, Fig. 7); the results are illustrated in Fig. 22:

The profile trend shown in Fig. 22 clearly indicates a unique linear relationship between both the quantities "N_A" and "$(D_{AM}/K\delta)_{SW}$". Since both these parameters, respectively, represent the salt transport "rate" and "magnitude" through the SWRO membrane during RO, which also substantiates further the authenticity of the flow transport model developed in this paper.

6.6. M

Owing to their relevance to salt concentration in the vicinity of membrane surface on the high pressure side of the membrane during RO, the effect of changes in X_{A2} values (Fig. 6) on the behaviour of concentration polarisation modulus (M) values (Fig. 10) was investigated and the results are presented in Fig. 23.

The results in Fig. 23 indicate that as salt content within the boundary solution film at the high pressure side of the membrane surface (X_{A2}) had risen, it caused concentration polarisation modulus to grow in magnitude thus resulting in a gradual lowering of permeate flow rate through the film of highly concen-

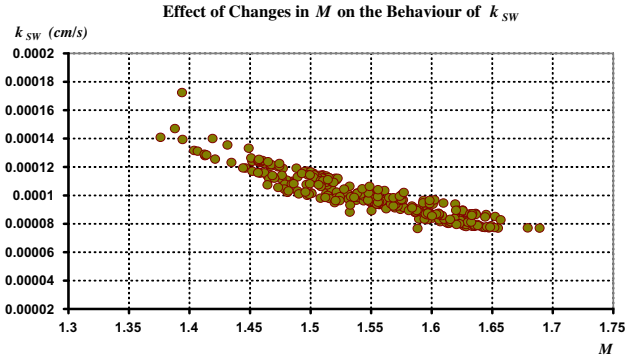

Fig. 24. Effect of changes in the concentration polarisation modulus on the high pressure side of the membrane surface (M) on the behaviour of mass transfer coefficient for seawater feed (k_{SW}).
Note: As with the results obtained in Fig. 21, Fig. 24 results similarly indicate that as concentration polarisation modulus was intensifying, the mass transfer coefficient decreased hence impeding transport of pure water through the concentrated film to the RO membrane.

trated salt solution at membrane surface and through the membrane (earlier shown in Fig. 17). Effect of changes in the quantity M values was also investigated against those of k_{SW} so as to study the behaviour of k_{SW} at the increasing trend of M during this SWRO process (Fig. 24).

6.7. l

The quantity l (concentrated solution film (boundary layer) thickness on the high pressure side of the membrane) is with fundamental relevance to four quantities "l, X_{A2}, k_{SW} and M" (as all the four parameters are associated with concentrated boundary solution at the high pressure side of the RO membrane) and have direct effect on the permeate flow rate

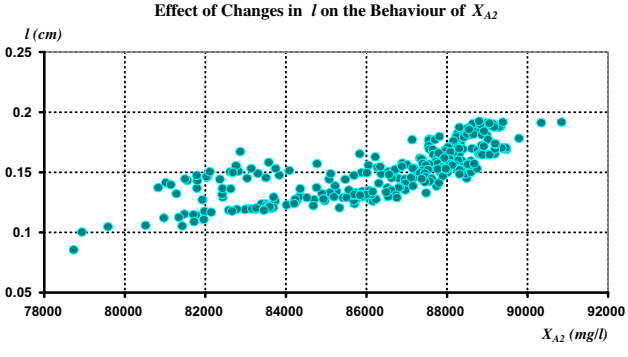

Fig. 25. Effect of changes in the concentrated solution film (boundary layer) thickness on the high pressure side of the membrane (l) on the behaviour of X_{A2}.

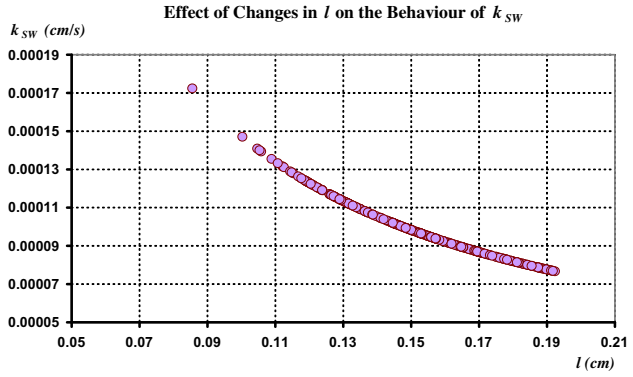

Fig. 26. Effect of changes in the concentrated solution film (boundary layer) thickness on the high pressure side of the membrane (l) on the behaviour of k_{SW}.

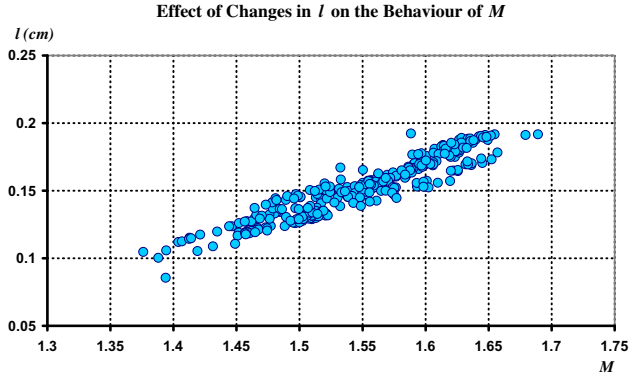

Fig. 27. Effect of changes in the concentrated solution film (boundary layer) thickness on the high pressure side of the membrane (l) on the behaviour of M.

through the RO membrane. The effect of changes in quantity l (from Fig. 11) on the behaviour of X_{A2}, k_{SW} and M was studied (Figs. 25–27):

The findings illustrated in Figs. 25–27 (as with the findings in Figs. 21, 23 and 24) together demonstrate that there exists a linear relationship of proportional similarity between these four quantities l, X_{A2}, k_{SW} and M, which is an expected functional characteristic since these quantities have direct relevance to salt content within the solution matrix contained on the high pressure side of the RO membrane.

6.8. ΔP

The varying effective pressure (ΔP) values from Fig. 12 were analysed against changes in seawater feed temperature (Fig. 5), as illustrated in Fig. 28.

The profile in Fig. 28 shows a gentle steady increasing linear trend followed by a steep decrease in ΔP values transpired when the seawater feed

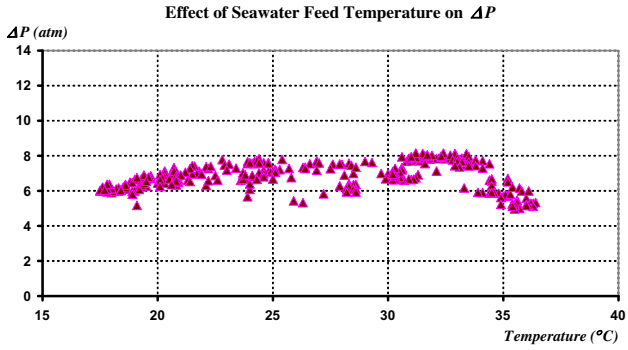

Fig. 28. Effect of seawater feed temperature on the effective pressure (ΔP).

temperature increased around 34°C (and beyond). This behaviour indicated that when the overall porosity of the SWRO membrane under study increased at the higher seawater feed temperature (as confirmed by the results for the quantity A in Fig. 14) it caused the effective pressure (ΔP) of the SWRO system to decrease by a corresponding degree of change.

7. Concluding remarks

The principal parameters that were determined from the derived correlations through this modelling analysis (primarily: A, X_{A2}, $(D_{AM}/K\delta)_{SW}$, k_{SW}, M and l) are all fundamental quantities that are essential in any seawater RO process operation and are valid for the seawater RO system examined in this case study that apply to the prevailing operating and seasonal conditions at the time of examination.

It is undeniable that concentration polarisation (M) has detrimental effects on the performance of any SWRO membrane process, with its magnitude being of a vital importance (though not been determined before as no literature cited). Likewise, the resulting concentrated boundary film thickness (l) and the salt concentration of boundary solution (X_{A2}) on the high pressure side of the membrane are as essential parameters as M that were also determined by the model in the overall application of this modelling analysis. These quantities are unique for being relevant to the concentrated boundary solution on the high pressure side of the RO membrane during RO.

Some expressions developed in this flow transport modelling analysis for establishing variations in the transport of feed species (water and salt) within the SWRO membrane module may be recognisable to specialists in the field. However, model concept and results achieved through its application using actual operation data presented the model with an essence of innovation and originality.

Symbols

1	—	subscript representing "bulk/feed solution"
2	—	subscript representing "concentrated boundary solution"
3	—	subscript representing "membrane permeated product solution"
A	—	subscript representing "salt"
A	—	pure water permeability constant (g-mol-H_2O/cm^2 s atm)
B	—	subscript representing "water"
c_1	—	molar density of feed solution (g-mol/cm^3)
c_2	—	molar density of concentrated boundary solution (g-mol/cm^3)
c_3	—	molar density of permeated product solution (g-mol/cm^3)
c	—	molar density of solution (assumed constant for seawater feed (g-mol/cm^3))
c_M	—	molar density of solution in membrane phase (g-mol/cm^3)
c_{M2}	—	molar density of solution in equilibrium with c_2 (g-mol/cm^3)
c_{M3}	—	molar density of solution in equilibrium with c_3 (g-mol/cm^3)
D_{AB}	—	diffusivity of salt in water; in this case study D_{AB} represents the diffusivity of salt inthe feed solution (which is seawater) (cm^2/s)
D_{AM}	—	diffusivity of salt in membrane phase (cm^2/s)
$(D_{AM}/K\delta)$	—	solute transport parameter (cm/s)
$(D_{AM}/K\delta)_{SW}$	—	solute (salt) transport parameter for the seawater feed (cm/s)
day	—	RO membrane operating day
K	—	proportionality constant relating "X_A and X_{AM}"
k	—	mass transfer coefficient on the high pressure side of the membrane (cm/s)
k_{SW}	—	mass transfer coefficient for the seawater feed (cm/s)
l	—	thickness of concentrated boundary solution film on the high pressure side of the membrane (cm)
M	—	magnitude of the concentration polarisation modulus
M	—	subscript representing "membrane phase"
M_B	—	molecular weight of water (assumed to equal 18.015 [18], where the atomic mass of Hydrogen (H) = 1.008 and Oxygen (O) = 15.999

m — solute molality in the seawater feed solution (obtained from data available in the literature [17] for the properties of seawater at 25°C (as 0.550)

N_A — solute flux through the SWRO membrane pores (g-mol/cm^2 s)

N_B — water flux through the membrane pores (g-mol/cm^2 s)

P — operating (gauge) pressure on the high pressure side of membrane (atm)

[PWP] — pure water permeability (permeation rate) through the effective area of membrane surface (g/h)

ΔP — effective pressure (constitutes the driving force for water flow through the membrane pores during RO; from a practical standpoint it represents the portion of feed pressure in excess of the osmotic pressure of feed solution ($\pi(X_{A1})$) corresponding to the feed solution concentration (X_{A1}) in an RO process) (atm)

Q_1 — volumetric feed flow rate for single SWRO module (m^3/h)

Q_3 — volumetric permeate flow rate for one single SWRO membrane module (m^3/h)

RS_B — rate of water separation or conversion rate (%)

S — effective area of membrane surface (cm^2)

S-Design — design surface area of the examined SWRO membrane bundle; provided by DuPont [15] (as 424 m^2)

X_A — mole fraction (concentration) of salt in solution phase (as mg/l)

X_{A1} — mole fraction of feed solution

X_{A2} — mole fraction (salt concentration) of the concentrated boundary solution

X_{A3} — mole fraction of permeated product solution

X_{AM} — mole fraction (concentration) of salt within membrane phase

X_{AM2} — mole fraction of salt in membrane phase (X_{AM}) in equilibrium with X_{A2}

X_{AM3} — mole fraction of salt in membrane phase (X_{AM}) in equilibrium with X_{A3}

z — distance in the coordinate set in boundary layer vertical to membrane surface (cm)

$\Delta\pi$ — (1) osmotic pressure differential across the fibre membrane (Bar) and (2) difference between osmotic pressure of solution on high pressure side and low pressure side of membrane (Bar)

π_b — osmotic pressure of concentrated boundary solution directly at the membrane surface on the high pressure side of the membrane (but not necessarily in contact with the membrane surface as a layer of preferentially sorbed pure water layer exists (Bar)

π_P — osmotic pressure of permeate on the low pressure side of the membrane (Bar)

$\pi(X_A)$ — osmotic pressure of solution corresponding to salt mole fraction X_A (atm)

$\pi(X_{A2})$ — osmotic pressure of concentrated boundary solution on the high pressure side of the membrane corresponding to the salt mole fraction X_{A2} (atm)

$\pi(X_{A3})$ — osmotic pressure of permeated product solution on the low pressure side of the membrane corresponding to the salt mole fraction X_{A3} (atm)

δ — (1) membrane thickness (m); (2) effective thickness of membrane (m) and (3) concentrated boundary layer thickness (m)

References

[1] S. Sourirajan, Reverse Osmosis, Transport Through Reverse Osmosis Membranes, Logos Press Limited Scientific Publications, Published by Unwin Brothers Limited, Surrey, England, 1970.

[2] (a) S. Kimura, S. Sourirajan, A. I. Ch. E. J., 13 (1967) 497; (b) S. Sourirajan, S. Kimura, Ind. Eng. Chem. Process Des. Dev., 6 (1967) 504; (c) S. Kimura, S. Sourirajan, Ind. Eng. Chem. Process Des. Dev., 7 (1968) 41–197, 539–548.

[3] J.P. Agrawal, S. Sourirajan, Ind. Eng. Chem. Process Des. Dev. 8 (1969) 439.

[4] S. Sourirajan, in: S. Sourirajan (Ed.), Reverse Osmosis—A General Separation Technique, Reverse Osmosis and Synthetic membranes, Division of Chemistry, National Research Council Canada Publications, Ottawa, 1977, pp. 1–4.

[5] S. Sourirajan, T. Matsuura, Reverse Osmosis/Ultrafiltration Process Principles, Chapter 2—Transport Through Reverse Osmosis Membranes—Part I, National Research Council Canada Publications, Division of Chemistry, Ottawa, 1985.

[6] S. Sourirajan, Reverse Osmosis, Chapter 1: General Applicability of the Technique, Division of Applied Chemistry, National Research Council of Canada/Academic Press, Ottawa/New York, NY, 1970.

[7] S. Sourirajan, Reverse Osmosis, Chapter 3: Transport Through Reverse Osmosis Membranes, National Research Council of Canada/Academic Press, Ottawa/New York, NY, 1970.

[8] T. K. Sherwood, R.L. Pigford, Absorption and Extraction, McGraw Hill, New York, NY, 1952, p. 53.

[9] R.E. Terybal, Mass Transfer Operations, McGraw Hill, New York, NY, 1955, p. 38.

[10] T. Matsuura, S. Sourirajan, Reverse osmosis transport through capillary pores under the influence of surface forces, Ind. Eng. Chem. Process Des. Dev. 20 (1981) 273.

[11] T.K. Sherwood, Mass Transfer between phases, 33rd Annual Priestly Lectures, Pennsylvania State University, 1959, p. 38.
[12] Aqua-Chem, Inc., Conversion Factories & Data, Water Technologies Division, Designers and Manufacturers of Process and Desalting Systems, 2001.
[13] DuPont Company, General Guide to Products and Properties, Permasep Reverse Osmosis Products (Brochure, H-29527–1, Rev. 11/93, Printed in USA), 1993.
[14] Ahmed H. Hashim, Modelling Analysis to Predict Performance for a Seawater RO Membrane Module, (Manager, Addur SWRO Desalination Plant, Electricity and Water Authority, Kingdom of Bahrain), PhD, in: IDA World Congress—Atlantis, The Palm—Dubai, UAE, 7–12 November 2009 (REF: IDAWC/DB09-011).
[15] Verbal and Electronic Communications with DuPont technical representative on DuPont Permasep RO membrane products, Various Literature, Information and Data (Recommended and Design), 1997–2001.
[16] S. Sourirajan, Reverse Osmosis, Appendix II (page 563)—Table A-17 Data for the System [NaCl–H_2O] at 25 °C, Division of Chemistry, National Research Council of Canada, Ottawa, Logos Press Limited—Academic Press, New York, NY, 1970.
[17] B.M. Fabuss, A. Korosi, Thermodynamic properties of sea water and its concentrates, Desalination 2 (1967) 271–278.
[18] R.A. Alberty, F. Daniels, Physical Chemistry, Fifth Edition, John Wiley & Sons, New York, NY, 1979.